Delayed Rectifying and Calcium-activated K^+ Channels and Their Significance for Action Potential Repolarization in Mouse Pancreatic β-Cells

PAUL A. SMITH, KRISTER BOKVIST, PER ARKHAMMAR, PER-OLOF BERGGREN, and PATRIK RORSMAN

From the Department of Medical Physics, Gothenburg University, S-400 33, Gothenburg, Sweden; the Department of Medical Cell Biology, Uppsala University, S-751 23 Uppsala, Sweden; and the Department of Endocrinology, Karolinska Institute, Karolinska Hospital, S-104 01 Stockholm, Sweden

ABSTRACT The contribution of Ca^{2+}-activated and delayed rectifying K^+ channels to the voltage-dependent outward current involved in spike repolarization in mouse pancreatic β-cells (Rorsman, P., and G. Trube. 1986. *J. Physiol.* 374:531–550) was assessed using patch-clamp techniques. A Ca^{2+}-dependent component could be identified by its rapid inactivation and sensitivity to the Ca^{2+} channel blocker Cd^{2+}. This current showed the same voltage dependence as the voltage-activated (Cd^{2+}-sensitive) Ca^{2+} current and contributed 10–20% to the total β-cell delayed outward current. The single-channel events underlying the Ca^{2+}-activated component were investigated in cell-attached patches. Increase of $[Ca^{2+}]_i$ invariably induced a dramatic increase in the open state probability of a Ca^{2+}-activated K^+ channel. This channel had a single-channel conductance of 70 pS ($[K^+]_o$ = 5.6 mM). The Ca^{2+}-independent outward current (constituting >80% of the total) reflected the activation of an 8 pS ($[K^+]_o$ = 5.6 mM; $[K^+]_i$ = 155 mM) K^+ channel. This channel was the only type observed to be associated with action potentials in cell-attached patches. It is suggested that in mouse β-cells spike repolarization results mainly from the opening of the 8-pS delayed rectifying K^+ channel.

INTRODUCTION

Patch-clamp recordings from mouse pancreatic β-cells have revealed the existence of a delayed outward K^+ current (I_K) which is not sensitive to $[Ca^{2+}]_i$ (Rorsman and Trube, 1986; Zünkler et al., 1988). Together with the inward Ca^{2+} current this current is able to sustain action potentials in single β-cells (Rorsman and Trube, 1986). The delayed outward K^+ current arises from the activity of K^+ channels with an

Address reprint requests to Dr. Patrik Rorsman, Department of Medical Physics, Gothenburg University, Box 33031, S-400 33, Gothenburg, Sweden.
Dr. Smith's present address is University Laboratory of Physiology, Oxford University, Parks Road, Oxford OX1 3PT, England.

J. GEN. PHYSIOL. © The Rockefeller University Press · 0022-1295/90/06/1041/19 $2.00
Volume 95 June 1990 1041–1059

approximate single-channel conductance of 10 pS (K_V; Rorsman and Trube, 1986; Zünkler et al., 1988). Studies on tumoral RINm5F-cell have led to the suggestion that a sizeable fraction of the outward current underlying spike repolarization is due to the activation of Ca^{2+}- and voltage-dependent K^+ channels of large unitary amplitude (K_{Ca}; Findlay and Dunne, 1985; Velasco and Petersen, 1987). In the present study we have assessed the relative contributions of K_V and K_{Ca} to the delayed outward current in normal β-cells. Our results indicate that K_V plays a major role in action potential repolarization and that K_{Ca} might participate in this process.

METHODS

Preparation of Cells for Patch-Clamp Experiments

Pancreatic islets were isolated from NMRI mice by collagenase digestion and dispersed into single cells by treatment with trypsin or shaking in low Ca^{2+} solution as previously described (Rorsman and Trube, 1986). Cells were plated on Falcon petri dishes and maintained for 1–4 d in RPMI 1640 tissue culture medium supplemented with fetal calf serum (10% vol/vol), 100 μg/ml streptomycin, 100 IU/ml penicillin, 50 μg/ml gentamycin, and 5 mM glucose.

Electrophysiology

We used the whole-cell, outside-out and cell-attached configurations of the patch-clamp technique (Hamill et al., 1981). Pipettes were pulled from borosilicate and aluminosilicate glass (Hilgenberg, GmbH, Malsfeld, FRG), coated with Sylgard near their tips and fire-polished. They had resistances of 2–5 MΩ when filled with KCl solution. Currents were recorded using an EPC-7 patch-clamp amplifier (List Electronic, Darmstadt, FRG). Pulse protocols were generated by a microcomputer. Unless otherwise stated pulses were 500 ms long and applied at a rate of 0.33 Hz. Membrane potentials were recorded using the current-clamp mode of the whole-cell configuration. Data were stored on videotape using a VCR (SL-2000; Sony, Tokyo, Japan) and a modified digital audio processor (PCM-F1; Sony, Tokyo, Japan). All electrophysiological experiments were performed at room temperature (19–25°C).

Data Analysis

Records were digitized using a Labmaster ADC (Scientific Solutions, Solon, OH). Unless otherwise indicated, whole-cell currents were digitized at 400–500 Hz without prior filtering. Single-channel records were filtered at 1–2 kHz (−3 dB) using a 4- or 8-pole Bessel filter and digitized at 2–4 kHz. Leakage and capacity currents were removed by subtraction of the scaled response to an average of eight 20-mV depolarizing pulses (whole-cell experiments) or using sweeps that did not contain any channel openings (single-channel experiments). The digitized current values were used to form amplitude distribution histograms and the single-channel currents estimated by fitting Gaussians to the peak corresponding to one open channel. The value of the open probability (P_o) was estimated for each pulse assuming that the maximal number of channel superimpositions (N) corresponds to the actual number of channels within the patch. The single-channel amplitude (i) and zero-current level were determined by eye using cursors and the total current (I) during each 500-ms pulse was calculated by integration. P_o was then estimated using the equation:

$$P_o = I/(i \times N) \quad (1)$$

The reference potential for all measurements was the zero-current potential of the pipette before establishment of the seal. Potentials have not been corrected for liquid junction

potentials. Results are presented as mean values ± SEM for indicated number of experiments. Statistical significances were evaluated using Student's *t* test.

Solutions

The composition of the different extra- and intracellular media is given in Table I. 3 mM Mg-ATP was included in all intracellular media to suppress the ATP-dependent K^+ current (Rorsman and Trube, 1985; Trube et al., 1986). We chose to block Ca^{2+} influx by using the inorganic Ca^{2+} antagonist Cd^{2+} instead of organic Ca^{2+} antagonists such as D-600, since the effects of the latter compounds are not or only slowly reversible.

Measurements of the Cytoplasmic Free Ca^{2+} Concentration and Insulin Secretion

Pancreatic islets were isolated from obese hyperglycemic mice, disrupted into single cells, and cultured overnight as previously described (Arkhammar et al., 1986). Cell suspensions were

TABLE I

Composition of Media

	Extracellular				Intracellular	
	A	B	C		D	E
NaCl	138	113	—	KCl	125	150
KCl	5.6	30.6	146	NMG	—	—
$MgCl_2$	1.2	1.2	1.2	$MgCl_2$	1	1
$CaCl_2$	1.3–10.2	1.3–2.6	2.6	$CaCl_2$	2	≈0.01
HEPES	5	5	5	EGTA	10	0.1
$CoCl_2$	(5)	—	—	KOH	30	—
$MnCl_2$	(5)	—	—	HCl	—	—
$CdCl_2$	(0.2)	—	—	HEPES	5	5
pH	7.4	7.4	7.4	MgATP	3	3
	(NaOH)	(NaOH)	(KOH)	pH	7.15 (KOH)	7.15 (KOH)

Compositions of the different extracellular (A–C) and intracellular (D–E) media are given (in millimolar). In the extracellular media, pH was adjusted to 7.4 with NaOH or KOH and in the intracellular media, it was adjusted to 7.15 using KOH as indicated beneath the columns. The values within the parentheses indicate that the compound was not usually present, but was added at the concentration given when included. The free concentration of Ca^{2+} was calculated as 0.06 μM in all intracellular media, using the binding constants of Martell and Smith (1974).

incubated in the presence of 1 μM fura-2/acetoxymethyl ester (Sigma Chemical Co., St. Louis, MO) during 45 min and subsequently loaded into a microflowcell. Briefly, a glass capillary with a volume of 30 μl was filled with fura-2–loaded cell aggregates mixed with Bio-Gel P4 polyacrylamide beads (Bio-RAD, Richmond, CA). The microcolumn was fixed and placed in the thermostatted cuvette compartment of a spectrofluorometer (LS5; Perkin-Elmer, Beaconsfield, UK). The flowcell was perfused with extracellular solution A (containing 1.3 mM Ca^{2+} and supplemented with 1 mg/ml albumin) either at +37°C or at room temperature (20–22°C). The excitation wavelengths were 340 and 380 nm and the emitted light was recorded at 510 nm. The flow rate in the system was 150 μl/min and the perfusate was collected in 1-min fractions and assayed for insulin using crystalline rat insulin as the standard. The 340/380 fluorescence ratio directly reflects the cytoplasmic free Ca^{2+} concentration

($[Ca^{2+}]_i$) and absolute values can be calculated if the ratios at saturating (R_{max}) and very low Ca^{2+} concentrations (R_{min}) are known (Grynkiewicz et al., 1985). However, these values represent averages for the whole cell and might underestimate changes in $[Ca^{2+}]_i$ just beneath the plasma membrane, which are of importance for channel regulation.

RESULTS

Biphasic Inactivation of I_K

The pancreatic β-cell has previously been shown to possess a delayed rectifying K^+ current ($I_{K,V}$) which is little affected by the intracellular Ca^{2+} concentration (Rors-

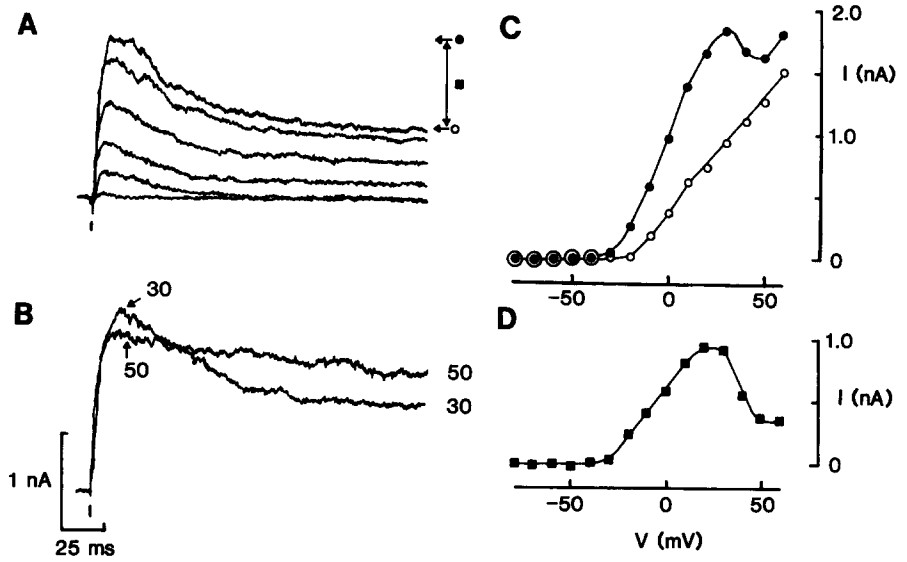

FIGURE 1. Two inactivation components of I_K. (*A*) Currents evoked by 200-ms depolarizations (rate 0.5 Hz) from −90 mV to (from bottom to top) −30, −20, −10, 0, +10, and +20 mV. Note the presence of inactivating and noninactivating components. (*B*) Currents observed during depolarizations to +30 and +50 mV. Note that the peak current is larger during the pulse to +30 mV and that current inactivates little during the depolarization to +50 mV. (*C*) *I-V* relationship for the peak (•) and sustained (○) I_K current amplitudes, measured as indicated in *A*. (*D*) *I-V* relationship of the inactivating current (■), which was measured as the difference between the peak current and the sustained current as indicated in *A*. Currents in this figure were recorded from a cell with an unusually large inactivating component. The pipette was filled with intracellular solution D and the bath contained extracellular medium A with 2.6 mM Ca^{2+}.

man and Trube, 1986) and removal of extracellular Ca^{2+} (Zünkler et al., 1988). $I_{K,V}$ has previously been shown to inactivate monoexponentially with a time constant of several seconds (Rorsman and Trube, 1986). However, careful inspection of the current records reveals the presence of an additional current component in >50% of the cells which inactivates completely within 100–200 ms. Fig. 1 shows currents recorded from a cell containing an unusually large fraction of the rapidly inactivat-

ing component. Outward currents were first observable during a depolarization to −30 mV. With more positive voltage commands, both the peak and steady-state currents (measured at the end of the pulse) increase but the relative contribution of the inactivating component becomes progressively smaller. During depolarizations to voltages beyond +30 mV the inactivating current decreases whereas the steady-state current still increases. At +50 mV the current response almost entirely consists of the noninactivating component. Fig. 1 *C* shows the current-voltage (*I-V*) relationships of the peak (•) and the sustained currents (○). Whereas the peak current shows an N-shaped *I-V* with a trough at +35 mV, the sustained current increases linearly with the applied voltage. Fig. 1 *D* shows the *I-V* of the difference between the peak and sustained currents corresponding to the inactivating component (■). This produces a bell-shaped curve that is small at voltages more negative than −30 mV, maximal at ~+20 mV, and then decreases at more positive potentials. These voltages are roughly similar to those previously reported for the Ca^{2+} current in

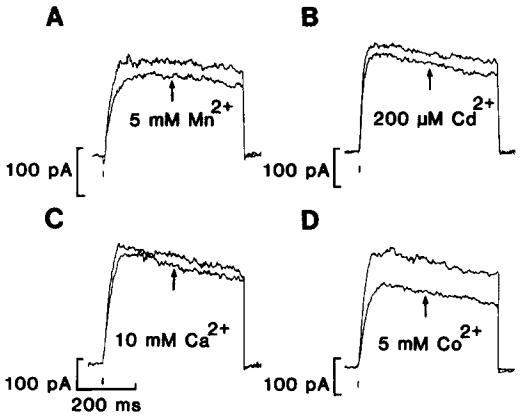

FIGURE 2. Effects of divalent cations on β-cell $I_{K,V}$. Depolarizing pulses were applied from a holding potential of −89 mV to +3 mV under control conditions and after inclusion of 5 mM Mn^{2+} (*A*), 200 μM Cd^{2+} (*B*), 7.6 mM Ca^{2+} (total: 10.2 mM; *C*), and 5 mM Co^{2+} (*D*). In each case the control record is of larger amplitude. Onset of depolarizing pulse is indicated by the vertical bar underneath the current traces. Different cells were used for each experiment. Pipette solution was intracellular medium E and control solution was the standard extracellular medium A containing 2.6 mM Ca^{2+}.

mouse β-cells (Rorsman and Trube, 1986; Plant, 1988) suggesting that it is produced by Ca^{2+} influx. It should be emphasized that most cells had much smaller inactivating components than those illustrated here and the contribution of the Ca^{2+}-activated K^+ current ($I_{K,Ca}$) to the β-cell I_K could not be assessed this way.

Effects of Inorganic Ca^{2+} Channel Blockers and Increasing Extracellular Ca^{2+} on $I_{K,V}$

The experiments in Figs. 2 and 3 were performed to develop the conditions to separate $I_{K,Ca}$ from the total outward current with minimal interference with $I_{K,V}$. These experiments were performed on cells in which $I_{K,V}$ predominated as evidenced by the absence of a rapidly inactivating component (cf. Fig. 1). Fig. 2 shows the effects of applying inorganic Ca^{2+} channel blockers and also of increasing extracellular Ca^{2+} concentration on $I_{K,V}$. The addition of Co^{2+} and Mn^{2+} at concentrations necessary to block the Ca^{2+} current (5 mM; Rorsman and Trube, 1986) both significantly

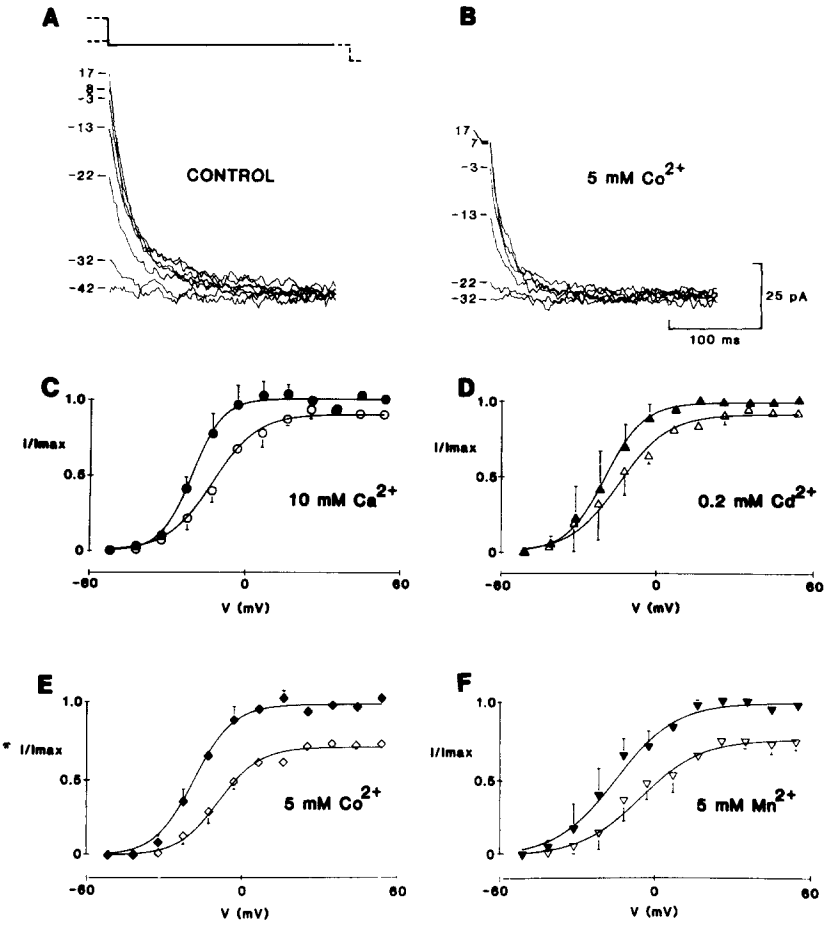

FIGURE 3. Effects of divalent cations on $I_{K,V}$ activation. (*A*, *top*) Schematic pulse protocol. The cell was clamped for 200 ms to different test potentials (V) between −52 and +55 mV. After each test pulse the cell was held for 400 ms at −51 mV. Pulse rate: 0.2 Hz. Holding potential between pulses: −88 mV. (*A*, *bottom* and *B*) Tail currents, recorded in control solution (*A*) and after addition of 5 mM Co^{2+} (*B*), elicited by pulses to the test potentials indicated to the left of the traces. Exponential curves (not shown) were fitted to the tail currents to determine initial amplitudes. Note reduction in tail current amplitudes as well as a voltage shift after the addition of Co^{2+}. (*C–F*) Activation curves in control solution (*filled symbols*) and after the addition of 7.6 mM Ca^{2+} (○), 0.2 mM Cd^{2+} (△), 5 mM Co^{2+} (◇), and 5 mM Mn^{2+} (▽). Normalized tail current amplitudes (I/I_{max}) are plotted vs. the potential (V) of the test pulse. Values are means ± SEM of three (*D* and *F*) or five (*C* and *E*) experiments. The sigmoidal curves were drawn by fitting the mean values of the data points to Eq. 2. The average of points corresponding to the three most depolarized potentials in the control solution was taken as unity (I_{max}). Control solution was the standard extracellular solution A containing 2.6 mM Ca^{2+}. The pipette contained intracellular solution D. The effects on the current gating were analyzed in cells with minimal Ca^{2+}-dependent K^+ current components (no rapidly inactivating current).

reduced $I_{K,V}$. Similar effects, although less pronounced, were observed when adding 0.2 mM Cd^{2+} and surprisingly when increasing the extracellular Ca^{2+} concentration to 10.2 mM. The latter effect could be interpreted in terms of a shift in the gating of $I_{K,V}$. It is well known that increasing the Ca^{2+} concentration shifts the activation of voltage-dependent currents towards more depolarized voltages (Hille, 1984) and it is therefore essential to investigate the effects of the divalent cations on the gating of $I_{K,V}$.

Effects of Divalent Cations on $I_{K,V}$ Activation

The effects of the divalent cations on the gating of $I_{K,V}$ were explored using a standard two-pulse protocol. Outward currents were elicited by voltage pulses going to potentials between −52 and +55 mV. The cell was subsequently clamped at −50 mV to reveal outward tail currents. Fig. 3 shows the tail currents obtained after pulses to voltages between −42 and +17 mV under control conditions (*A*) and after addition of 5 mM Co^{2+} (*B*). It can be seen that Co^{2+} induces a shift of ≈10 mV in the positive direction. Whereas half-maximal activation is seen at ~−20 mV under control conditions, a pulse to −10 mV is necessary to evoke a similar response in the presence of Co^{2+}. The results of several experiments in control solution and after addition of Ca^{2+} (final concentration, 10 mM), Cd^{2+} (0.2 mM), Co^{2+} (5 mM), and Mn^{2+} (5 mM) are shown in Fig. 3, *C–F*. The data points of the individual experiments under control and test conditions were fitted to the Boltzmann distribution:

$$I/I_{max} = \{1 + \exp[(V_h - V)/k]\}^{-1} \quad (2)$$

where I is the tail current amplitude, I_{max} is the maximal tail current, V is the voltage during the depolarizing pulse, V_h is the membrane potential at which 50% activation is attained, and k is the slope factor. Under control conditions, values of V_h and k of −19 ± 2 mV and 8.01 ± 0.95 mV, respectively (n = 5) were obtained. This value of V_h is similar to that previously reported (Rorsman and Trube, 1986). The effects of the divalent cations on these parameters are summarized in Table II. It can be observed that all ionic modifications shift the gating of the outward current by 5–10 mV towards more depolarized voltages. It should be noted that Mn^{2+} and Co^{2+} reduced the maximal tail current amplitude. This might reflect a direct blocking action of the high concentrations of these divalent cations on the delayed rectifying K^+ channels. For the further characterization of the $I_{K,Ca}$, Cd^{2+} (50–200 μM) was used because it causes the least interference with the gating of $I_{K,V}$.

Isolation of $I_{K,Ca}$

In Fig. 4 the Ca^{2+}-dependent outward K^+ current is separated from the total delayed outward K^+ current using 200 μM Cd^{2+}. In this cell the current thus obtained rapidly activates (within 20 ms) and inactivates (within 100 ms). The *I-V* relationships obtained in the control solution, after adding Cd^{2+} and after subtraction, are shown in Fig. 4 *B*. The Cd^{2+}-sensitive current is small at voltages more negative than −30 mV, maximal at ~+20 mV, and then decreases at more positive potentials with an extrapolated "reversal" at ~+70 mV. These voltages are coincident with those previously reported for the Ca^{2+} current in mouse β-cells (Rorsman

TABLE II

Activation Parameters for the Delayed Rectifier and Effects of Divalent Cations

Ion	Concentration	n	ΔV_h	Δk	ΔI_{max}
			mV	*mV*	*pA*
Ca^{2+}	10.2	5	7.6 ± 1.3*	0.55 ± 1.10	−5.5 ± 1.6*
Mn^{2+}	5	3	9.0 ± 2.6	1.18 ± 0.11‡	−11.5 ± 0.1‡
Co^{2+}	5	5	7.9 ± 1.8‡	0.46 ± 0.21	−10.4 ± 2.5*
Cd^{2+}	0.2	3	4.2 ± 2.1	0.51 ± 0.70	−2.0 ± 1.2

*$P < 0.05$ and ‡$P < 0.01$ (vs. control) as evaluated using Student's t test.

and Trube, 1986; Plant, 1988). This component is observable as a convexity of the control *I-V* relationship in 70% of the cells ($n = 54$). More than 75% of such cells also displayed a rapidly inactivating time course of the current response (cf. Fig. 1). Both the convexity of the *I-V*'s and the inactivating current component disappeared within 10–15 min. This time course is similar to that of the rundown of the Ca^{2+} current under these experimental conditions. The Cd^{2+}-sensitive K^+ current is relatively small and amounts to only 10–20% of the total outward current at +20 mV.

With high intracellular EGTA, $[Ca^{2+}]_i$ transients can be expected to be suppressed resulting in attenuation of the K_{Ca} responses. In a series of experiments we therefore used 0.1 mM EGTA (intracellular solution E). This did not lead to an increase in K_{Ca} contribution. It was ascertained in separate experiments that the

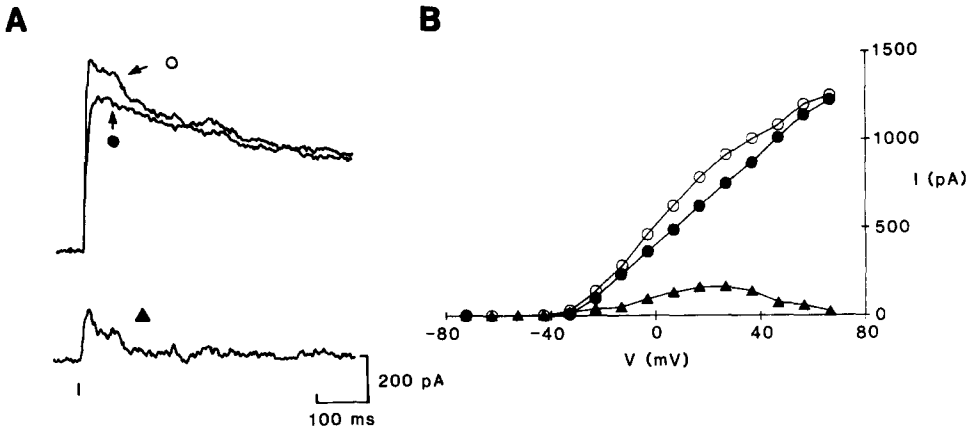

FIGURE 4. Separation of $I_{K,Ca}$ from total outward current. (*A*, *top*) Outward currents recorded in extracellular solution A containing 10.2 mM Ca^{2+} and after addition of 0.2 mM Cd^{2+} during depolarizing voltage pulses to +16 mV from a holding potential of −92 mV. The current response obtained in the Cd^{2+}-containing solution (•) was subtracted from the control (○) and the resulting difference was calculated ($I_{K,Ca}$; ▲). The onset of the depolarizing pulse is indicated by the vertical bar. The bath contained extracellular solution A containing 10.2 mM Ca^{2+}. The pipette was filled with intracellular solution D. (*B*) Peak *I-V* relationships representing the current observed in the control solution (○), after addition of 0.2 mM Cd^{2+} (•) and the resulting difference ($I_{K,Ca}$; ▲). Note that the convexity on the *I-V* relationship seen in the control solution disappears after addition of Cd^{2+}. The difference corresponds to the bell-shaped curve with a maximum at ~+20 mV.

β-cell retains voltage-dependent Ca^{2+} currents under the latter experimental conditions.

Effects of High External K^+ on the Cytoplasmic $[Ca^{2+}]_i$ and Insulin Release

To study the type of K^+ channel, which is activated by Ca^{2+} influx and thus underlies $I_{K,Ca}$, single-channel activity was recorded from cell-attached patches before and after elevation of $[Ca^{2+}]_i$. $[Ca^{2+}]_i$ was increased by increasing $[K^+]_o$ to 31 mM, which depolarizes the β-cell and results in the opening of voltage-dependent Ca^{2+} channels, producing an increase of $[Ca^{2+}]_i$ into the micromolar range (Arkhammar et al.,

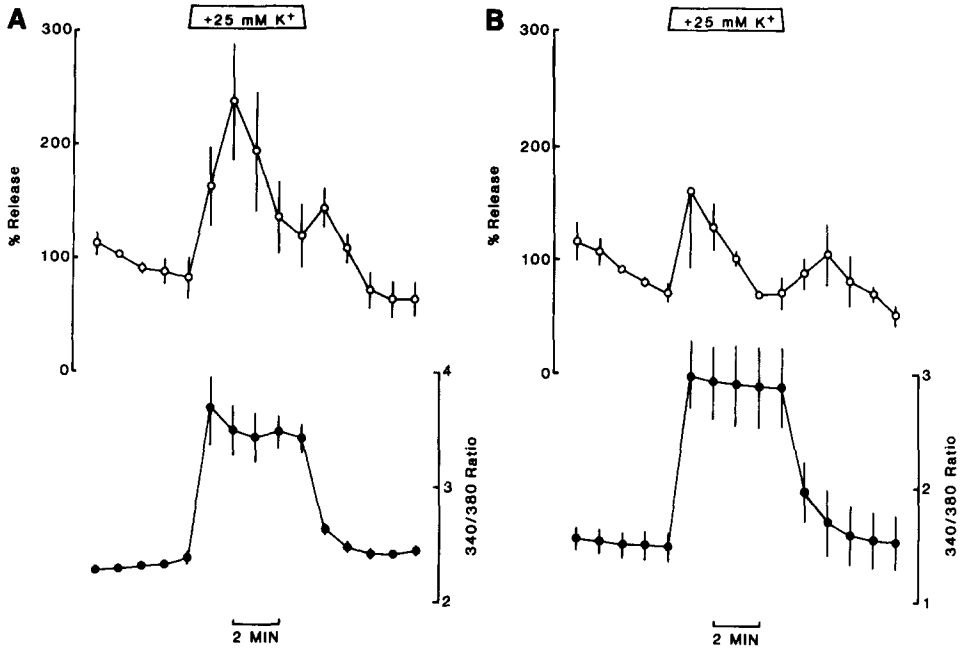

FIGURE 5. $[Ca^{2+}]_i$ and insulin release in perfused islet cell aggregates. (*A*) Insulin release (○) and changes in 340/380 ratio (●) at 37°C before and after the addition of 25 mM K^+ (final concentration, 30.6 mM). (*B*) Insulin release (○) and changes in the 340/380 ratio (●) at room temperature. The mean insulin level in the first five fractions was taken as 100% and consecutive values are given relative to this value. Changes in the 340/380 fluorescence ratio denote changes in $[Ca^{2+}]_i$ (see Methods). Extracellular solutions A and B containing 1.3 mM Ca^{2+} were used. Mean values ± SEM of four (*A*) and three (*B*) experiments.

1987). This increase is of a magnitude similar to that obtained when the β-cells are exposed to 20 mM glucose (Rorsman et al., 1984; Arkhammar et al., 1987). As shown in Fig. 5 *A*, $[Ca^{2+}]_i$ increases promptly during a pulse to 31 mM $[K^+]_o$ (switching the extracellular medium from A to B), displaying a small peak during the first minute of stimulation and then attaining a somewhat lower steady-state level. Concomitant with the rise in $[Ca^{2+}]_i$ there was a stimulation of insulin secretion. When $[K^+]_o$ was subsequently lowered to the normal 5.6 mM, both $[Ca^{2+}]_i$ and insulin release returned to prestimulatory levels within 2–4 min. When the experiments

were performed at room temperature (to permit direct comparison with the patch-clamp experiments), stimulation with high $[K^+]_o$ induced a pronounced increase in $[Ca^{2+}]_i$ similar to that obtained at 37°C. Upon reduction of the K^+ concentration to the normal 5.6 mM, $[Ca^{2+}]_i$ returned to the prestimulatory level, although at a somewhat slower rate than at 37°C. Despite the fact that the changes in $[Ca^{2+}]_i$ were virtually the same at 37°C and at room temperature, there was a marked reduction in insulin release under the latter conditions (cf. Atwater et al., 1984). However, high K^+ still promoted some stimulation of insulin release even at the lower temperature.

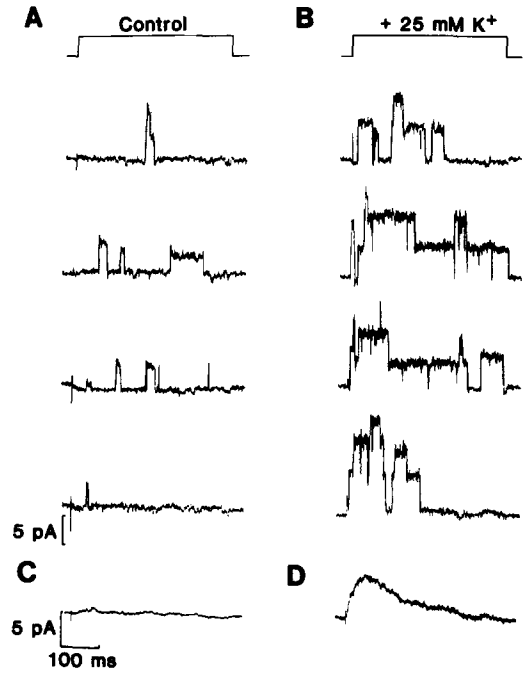

FIGURE 6. Effects of increasing $[Ca^{2+}]_i$ on K_{Ca} activity in a cell-attached patch. (*A*, *top*) Schematic pulse protocol. Depolarizing voltage pulses going from the resting potential (~−70 mV) to an estimated membrane potential of +20 mV. (*A*, *bottom*) Channel activity under control conditions. Rare openings of K_{Ca} were observed. (*B*, *top*) Schematic pulse protocol. In order to compensate for the change in membrane potential when increasing $[K^+]_o$, the patch potential was increased by 30 mV (*B*, *bottom*) Channel activity observed after increase of $[Ca^{2+}]_i$. (*C–D*) Associated mean currents obtained under basal conditions (*C*; 28 sweeps with channel openings and 20 zero sweeps) and after increase of $[K^+]_o$ (*D*; 74 sweeps with channel openings and 4 zero sweeps). Note dramatic increase of current after elevation of $[Ca^{2+}]_i$. The pipette contained normal extracellular solution A (2.6 mM Ca^{2+}) and the bath contained extracellular media A and B (2.6 mM Ca^{2+}).

K_{Ca} Activity Evoked by Increased $[Ca^{2+}]_i$ in Cell-Attached Patches

Fig. 6 shows K^+ channels recorded during depolarizations to ~+20 mV in the standard extracellular solution and after raising $[Ca^{2+}]_i$ by elevation of extracellular K^+. These experiments were performed in cell-attached patches to avoid the problem with rundown of the Ca^{2+} channels, which takes place in isolated patches making it difficult to quantitatively study the effects of Ca^{2+} influx on K_{Ca} activity. Openings of K_{Ca} are rare under basal conditions. Most sweeps contained openings of a K^+ channel with an amplitude of ~0.5 pA, which probably corresponds to the 10-pS

channel seen in outside-out patches (see Fig. 10, below). After the increase of $[Ca^{2+}]_i$, the activity of K_{Ca} increases dramatically and occasionally as many as three to five simultaneous channel openings are observed (Fig. 6 *B*). This channel inactivates fairly rapidly and at the end of the 400-ms depolarization, channel openings were rarely observed. The associated mean currents are shown in Fig. 6, *C–D*. It is clear that, although activating and inactivating somewhat slower, the associated mean current obtained in high $[K^+]_o$ resembles the whole-cell $I_{K,Ca}$ (Figs. 1 and 4). In four cell-attached patches the average increase of the associated mean currents induced by elevation of $[K^+]_o$ corresponded to 5.5 ± 1.2 pA.

The patch potential is the sum of the cell's membrane potential and the voltage applied to the pipette. The gating of K_{Ca} is known to be highly voltage dependent (Cook et al., 1984; Velasco and Petersen, 1987). The single-channel current amplitude can be used to monitor changes in the membrane potential. In the control solution, the single-channel amplitude obtained from a Gaussian fit to the amplitude distribution histogram was 5.6 ± 0.9 pA ($n = 4$). After the increase of $[K^+]_o$ a value of 5.7 ± 0.3 pA ($n = 4$) was obtained. This indicates that the voltage sensed by the channel was the same under both experimental conditions and it can therefore be concluded that the observed stimulation of K_{Ca} activity is attributable to the increased $[Ca^{2+}]_i$.

The single-channel conductance of the channel activated by elevation of $[Ca^{2+}]_i$ was 72.5 ± 3.5 pS ($n = 3$) in the voltage range −30 to 30 mV. This value is close to that reported for a K^+ channel activated by Ca^{2+} influx in RINm5F-cells under comparable experimental conditions (Velasco and Petersen, 1987). An estimate of the single-channel K^+ permeability (P_K) was obtained by fitting the observed data points to the Goldman-Hodgkin-Katz (GHK) equation. The single channel P_K is then given by:

$$P_K = i \Big/ \frac{VF^2}{RT}\left[\frac{[K^+]_i \exp(VF/RT) - [K^+]_o}{\exp(VF/RT) - 1}\right] \quad (3)$$

where voltages are in volts and R, T, and F have their usual meanings. $[K^+]_i$ was assumed to be 120 mM (Meissner et al., 1978) and $[K^+]_o$ was 5.6 mM. A value of P_K of $3.1 \pm 0.2 \times 10^{-13}$ cm^3s^{-1} ($n = 3$) was obtained.

Effects of High $[Ca^{2+}]_i$ on Open Probability of K_{Ca}

The effects of increased $[Ca^{2+}]_i$ on the channel's open probability is summarized in Fig. 7 *A*. It can be observed that channel activity is low at normal $[K^+]_o$ ($P_o < 0.05$). After the increase of $[K^+]_o$ (and hyperpolarization of the patch by 30 mV; indicated by the trace in *B*), P_o increases dramatically and remains high throughout the elevation of $[K^+]_o$ (cf. Fig. 5). Upon removal of K^+, channel activity declines slowly and reaches original values within 5 min (not shown). This time course is comparable to that observed for the decrease in $[Ca^{2+}]_i$ upon return to normal $[K^+]_o$ (cf. Fig. 5 *B*).

$I_{K,V}$ Recorded with High $[K^+]_o$

We then turned to the question of which type of K^+ channel is involved in action potential repolarization. This can be established directly by recording K^+ channel

currents activated by action potentials in cell-attached patches. In the presence of normal ionic gradients, K^+ channels reverse at voltages close to the resting membrane potential and channel openings can only be visualized by depolarizing the patch. However, both $I_{K,V}$ and $I_{K,Ca}$ inactivate during sustained depolarization. Openings of K^+ channels activated by action potentials could therefore not be studied under these experimental conditions. The use of pipettes containing high $[K^+]$ facilitates the recording of K^+ channels at voltages close to the K^+ equilibrium potential. To enable direct comparison with the whole-cell currents it was essential to investigate the properties of $I_{K,V}$ when recorded in high $[K^+]_o$. Fig. 8, *A–B* shows $I_{K,V}$ recorded with normal 5.6 mM $[K^+]_o$ and after an increase to 146 mM, respectively. It can be observed that the currents show little rapid inactivation and it may therefore be assumed that these currents reflect predominantly the activity of $I_{K,V}$. With high $[K^+]_o$, depolarizations to negative potentials produce slowly activating

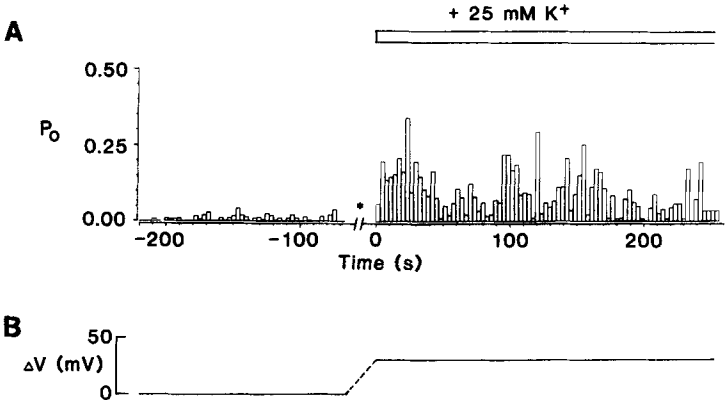

FIGURE 7. Effects of increased $[Ca^{2+}]_i$ on open probability of K_{Ca}. (*A*) Variation in P_o before and after increasing $[K^+]_o$ (indicated by the horizontal bar). The star (*) indicates a period of 60 s missing because of measurement of the single-channel *i-V*. The effect on P_o reversed slowly upon reduction of $[K^+]_o$. Same experiment as in Fig. 6. P_o was determined as described in text. *B* indicates the change in patch potential. After addition of 25 mM K^+, the patch was hyperpolarized by 30 mV to compensate for the depolarization.

inward currents. The currents become observable at voltages more negative than those required in the normal extracellular solution. However, this is probably not attributable to a shift in the activation properties. The whole-cell current (*I*) is given by the expression $I = NiP_{open}$ where N is the number of channels in the cell, i the single-channel amplitude, and P_{open} the open probability of the channel. As will be shown in Fig. 10, the single-channel currents at negative voltages are much smaller with normal $[K^+]_o$ than in the presence of 146 mM. The observed whole-cell currents will consequently be considerably larger in the latter solution despite a similar degree of channel activation. Fig. 8 *C* shows the *I-V* relationships of the currents recorded with normal extracellular solution (•) and after increase of $[K^+]_o$ to 146 mM (○). When recorded with the latter solution, $I_{K,V}$ reaches a maximum inward current at ~ -20 mV and then increases linearly with the applied voltage with a reversal at ~0 mV.

Time Course of $I_{K,V}$ Activation in Normal and High $[K^+]_o$

Fig. 9 compares the time course of $I_{K,V}$ activation in normal (5.6 mM; *A*) and increased $[K^+]_o$ (146 mM; *B*). As illustrated in Fig. 9, *A–B*, the activation of the K^+ currents could be described by n^2 kinetics where $n(t) = n_\infty[1\text{-exp}(-t/\tau)]$ (cf. Hille, 1984). The results of four experiments are summarized in Fig. 9 *C*. When recorded

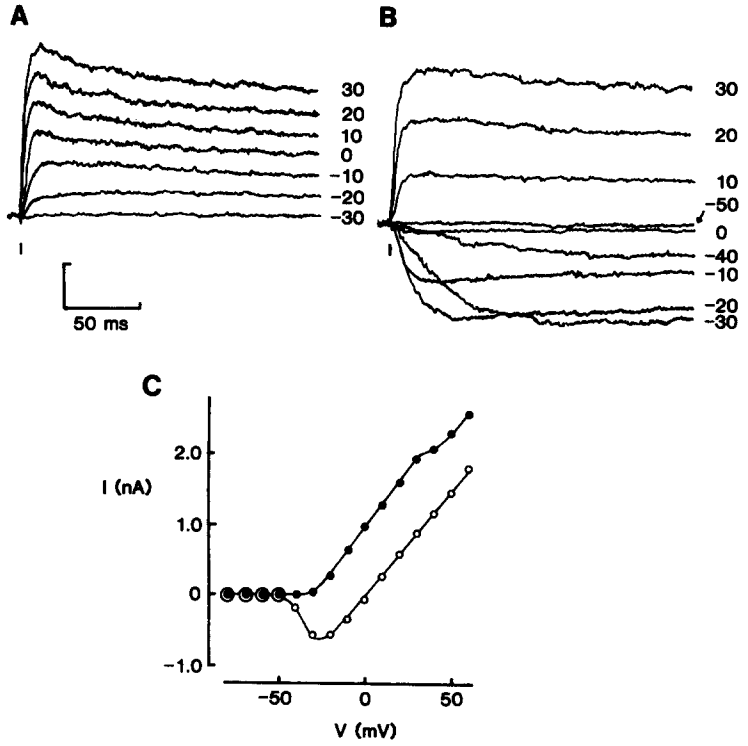

FIGURE 8. $I_{K,V}$ recorded with normal and high $[K^+]_o$. (*A*) $I_{K,V}$ recorded during 200-ms depolarizations (rate, 0.5 Hz) to the indicated potential in the presence of 5.6 mM $[K^+]_o$ (extracellular medium A with 2.6 mM Ca^{2+}]. (*B*) $I_{K,V}$ recorded from the same cell as in *A* after increasing $[K^+]_o$ to 146 mM (extracellular medium C). Note that depolarizations to negative potentials evoke inward currents. Scale bar corresponds to 500 pA in *A* and 250 pA in *B*. Note slow activation of inward currents. Onset of depolarizations is indicated by vertical bars underneath the current traces in *A* and *B*. This cell contained only a small $I_{K,Ca}$ as indicated by the absence of rapidly inactivating components. (*C*) *I-V* relationships recorded in *A* (•) and in *B* (○). The pipette contained intracellular solution D.

in the normal extracellular solution (○), the time constant of activation (τ) varied little in the voltage range −20 to +50 mV. Activation was two to three times slower in the presence of 146 mM (•) than in 5.6 mM $[K^+]_o$ at all voltages negative to +20 mV. Activation also showed more pronounced voltage dependence, being more rapid during larger depolarizations (cf. Fig. 8 *B*).

Single Delayed Rectifying K^+ Channels

Fig. 10 shows the single K^+ channel events observed during membrane depolarization in an outside-out patch. The most commonly observed channel had an amplitude of ~0.5 pA during pulses to 0 mV, when recorded with normal ionic gradients. Often as many as 10 simultaneous openings of this channel type were observed within the same patch. Typical sweeps containing this channel are shown in Fig. 10 *A*. The associated mean current produced by 97 sweeps is shown in Fig. 10 *B*. The current shows delayed activation (maximum reached within 50 ms) and does not inactivate much during the 500-ms depolarization. This behavior resembles that of the whole-cell $I_{K,V}$ (cf. Fig. 2), suggesting that the delayed rectifying whole-cell current flows through these channels. This conclusion is reinforced by the observa-

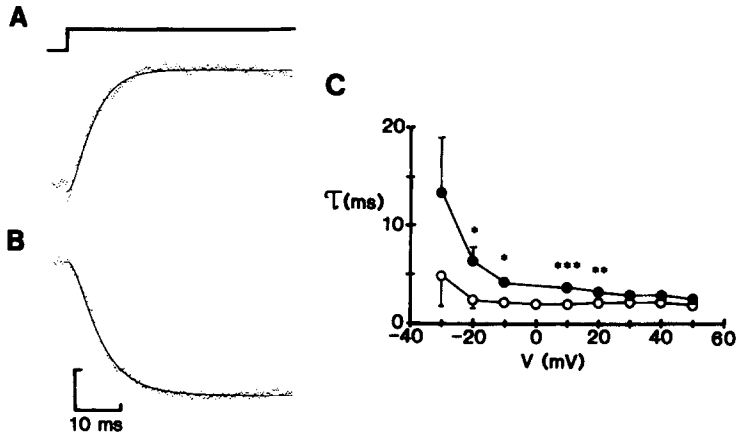

FIGURE 9. Time course of activation of $I_{K,V}$. (*A* and *B*) Currents evoked by depolarization to −10 mV (indicated by step in *A*) in the presence of (*A*) 5.6 mM and (*B*) 146 mM $[K^+]_o$. Points show original digitized data. Current signal was digitized at 4 kHz. Superimposed curves show expected time courses of activation assuming n^2 kinetics using time constants (τ_n) of 3.9 and 4.9 ms in *A* and *B*, respectively. Traces taken from the experiment in Fig. 8. Scale bar corresponds to 200 pA in *A* and 100 pA in *B*. (*C*) τ-*V* relationship recorded in 5.6 mM (○) or 146 mM $[K^+]_o$ (●). Mean values ± SEM of four experiments are given. $*P < 0.05$; $**P < 0.02$; $***P < 0.01$.

tion that the whole cell and these single-channel currents have the same sensitivity to the K^+ channel blockers tetraethylammonium (TEA) and quinine (Bokvist et al., 1990*a*). Fig. 10 *C* shows examples of inward K^+ currents recorded during depolarizations using pipettes containing ~150 mM K^+ (intracellular solution D). The single-channel current voltage (*i-V*) relationships recorded with $[K^+]_o$ of 5.6 mM (○) and 146 mM (●) are shown in Fig. 10 *D*. Approximation of the GHK equation (Eq. 3) to the data points indicated a P_K value of $2.8 \pm 0.1 \times 10^{-14}$ cm^3s^{-1} ($n = 15$) in 5.6 mM $[K^+]_o$. A linear slope conductance (γ) of 8.4 ± 0.3 pS ($n = 15$) was observed in the voltage range −40 to +50 mV with an extrapolated reversal at ~−60 mV. This value of γ is similar to those previously reported from cell-attached and outside-out patches (Rorsman and Trube, 1986; Zünkler et al., 1988). After $[K^+]_o$ increased to

146 mM, the reversal potential of the *i-V* relationship was shifted to 0 mV and γ increased to 15.5 ± 0.9 pS ($n = 7$) whereas P_K was not affected and averaged $2.8 \pm 0.2 \times 10^{-14}$ cm^3s^{-1} ($n = 7$).

K^+ Channels Activated by Action Potentials

Fig. 11 shows K^+ channels activated by an action potential in a cell-attached patch on a β-cell stimulated with 20 mM glucose. The top trace shows an example where a

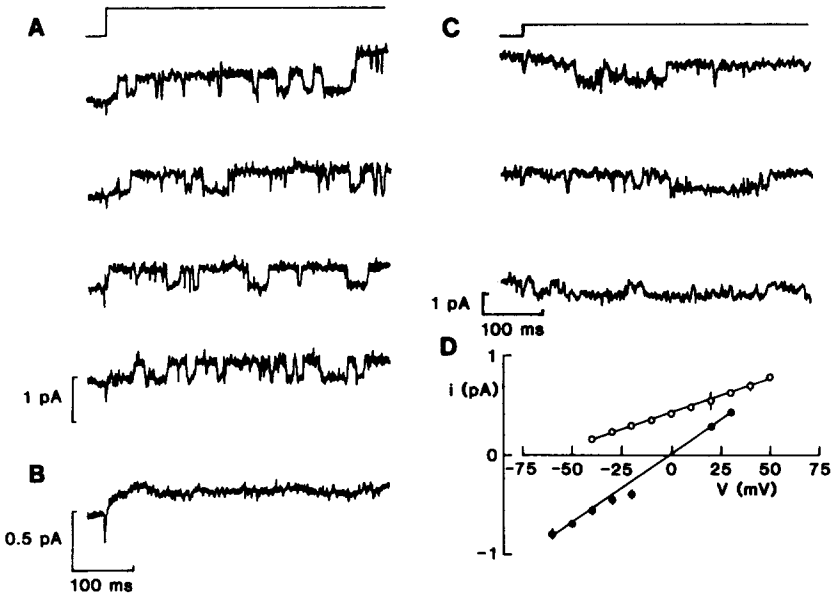

FIGURE 10. Single delayed rectifying K channels. (*A, top*) Schematic pulse protocol. Voltage pulses went to 0 mV from a holding potential of −70 mV. (*A, bottom*) Examples of channel openings. Channel openings are upward. Bath contained standard extracellular solution A (2.6 mM Ca^{2+}). (*B*) Associated mean current of 97 sweeps (49 sweeps containing channel openings and 48 zero sweeps). (*C*) Example of channel opening recorded during depolarizations to −50 (*top*), −40 (*middle*), and −30 mV (*bottom*) with the high $[K^+]_o$-solution (extracellular medium C). Channel openings are downward. (*D*) Single-channel *i-V* relationships obtained in 5.6 mM (○) and 146 mM $[K^+]_o$ (●). Mean values ± SEM (when larger than the size of symbols) for 3–11 (○) and 3–7 (●) experiments are shown. In the high-$[K^+]_o$ solution, channel amplitudes could not be accurately determined in the voltage range −20 to +10 mV and such openings were consequently not analyzed. The pipette was filled with intracellular solution D.

β-cell action potential (seen as a biphasic current deflection; cf. Fenwick et al., 1982) fails to activate channels within the patch. The lower three traces show examples where the passing of an action potential leads to the activation of one, two, and three channels. The current amplitude of the individual openings was measured during the "tail-current phase" when repolarization of the action potential was complete. A stable single-channel current amplitude of 0.7–0.8 pA was observed.

The interspike membrane potential of the cell was estimated to be −50 mV from the amplitude of an opening of the ATP-regulated K^+ channel. A similar value of the interspike voltage has been observed in current-clamp whole-cell recordings (Rorsman and Trube, 1986). The current amplitude of the channel activated by the action potentials is in good agreement with that observed for K_V in the outside-out patch experiments at a membrane potential of −50 mV (Fig. 10, *C–D*). It is evident that the channels start opening during the repolarization phase of the action potential. The exact onset of channel activation is difficult to determine since the single-

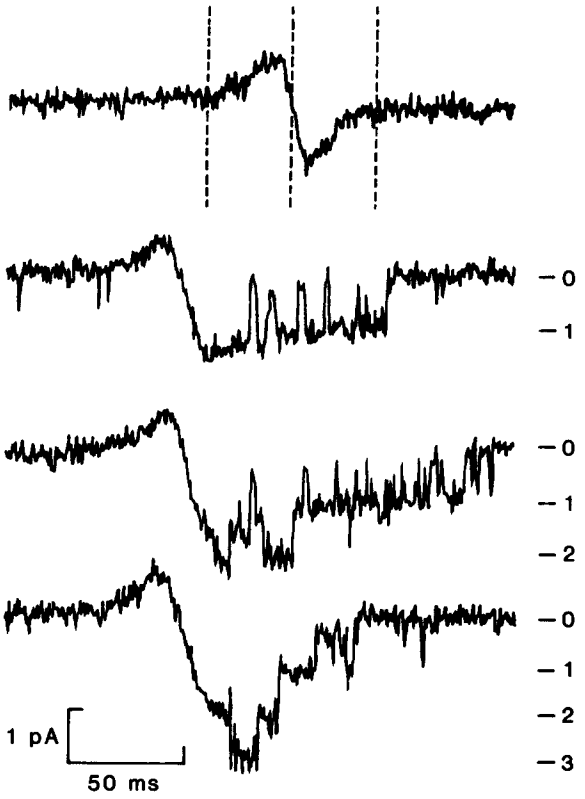

FIGURE 11. K^+ channels activated by action potentials. Biphasic current deflections corresponding to action potentials recorded from a cell-attached patch on a β-cell stimulated with 20 mM D-glucose. The parts of the action potential corresponding to the initiation (*left dashed line*), the peak (*middle dashed line*), and the end of the action potential (*right dashed line*) are indicated on the top trace, which shows an action potential not associated with K^+ channel openings. The lower three traces show examples where one to three channels are opened at the end of the biphasic current deflection. Currents are inward because of high $[K^+]_o$ (extracellular solution C) in the pipette. Bath contained standard extracellular medium A containing 2.6 mM Ca^{2+}.

channel K^+ currents reverse at about 0 mV with the present ionic gradients and will consequently be quite small at times corresponding to the peak of the action potential. However, the whole-cell experiments suggest that activation of K_V will be two to three times faster with normal extracellular $[K^+]_o$ (cf. Fig. 9 *C*). It is therefore likely that under physiological conditions K_V not only participates in but also initiates action potential repolarization. Other types of K^+ channels were never observed to be activated by action potentials. We therefore suggest that in normal β-cells spike repolarization results mainly from the opening of K_V.

DISCUSSION

Magnitude and Characteristics of $I_{K,Ca}$ in Pancreatic β-Cells

The voltage range where $I_{K,Ca}$ is observed overlaps that of the Ca^{2+} current recorded in β-cells, strongly suggesting that it is in fact activated by an influx of Ca^{2+}. However, $I_{K,Ca}$ is much less prominent in pancreatic β-cells than in many other cell types, where large Ca^{2+}-dependent humps are seen on the whole-cell *I-V* relationships (Heyer and Lux, 1976; Marty and Neher, 1985; Ritchie, 1987). In most β-cells the contribution of $I_{K,Ca}$ is reflected only as a small convexity on the *I-V* relationship. The Ca^{2+}-dependent component also did not increase when the internal Ca^{2+}-buffering capacity was reduced by lowering the concentration of EGTA to 0.1 mM. A similarly weak correlation between the size of $I_{K,Ca}$ and the concentration of EGTA has already been observed in chromaffin cells (Marty and Neher, 1985). Measurements of a Cd^{2+}-sensitive outward K^+ current component using the perforated patch whole-cell configuration (nystatin technique; Horn and Marty, 1988) indicated that even in the intact β-cell, $I_{K,Ca}$ does not contribute >10–20% to the delayed outward K^+ current (Smith, P.A., F.M. Ashcroft, and P. Rorsman, unpublished observations). $I_{K,Ca}$ inactivates completely within a few hundred milliseconds. It is therefore likely that the inactivating K^+ current component regularly observed in whole-cell recordings, at least in part, is attributable to $I_{K,Ca}$.

Roles of K_V and K_{Ca} in the β-Cell

K_{Ca} has been proposed to be involved in spike repolarization in insulin-secreting cells (Velasco and Petersen, 1987). Our present observation that depolarizing voltage pulses elicit openings of K_{Ca} after increasing $[Ca^{2+}]_i$, supports this idea. Analysis of the voltage noise associated with β-cell action potentials indicates a P_K of 3.6×10^{-13} cm^3s^{-1} for a channel activated during the action potential (Bangham et al., 1986; Bangham and Smith, 1987). This figure is very close to the 3.1×10^{-13} cm^3s^{-1} we now observe for K_{Ca} in cell-attached patches. However, the relative smallness of $I_{K,Ca}$ suggests that the participation of this current is not critical for action potential repolarization. In fact, the activity of K_{Ca} can be completely blocked by TEA^+ with little effect on glucose-induced electrical activity (Atwater et al., 1979; Bokvist et al., 1990*b*). We therefore propose that in mouse β-cells action potential repolarization is primarily due to $I_{K,V}$. This notion is supported by the direct demonstration that the delayed rectifying K^+ channel (K_V) is the only type of K^+ channel activated by action potentials in cell-attached patches on intact β-cells.

Financial support was obtained from the Swedish Medical Research Council (12X-08647 and 19X-00034), the Swedish Diabetes Association, the Nordisk Insulin Foundation, the Swedish Hoechst Diabetes Research Foundation, Åke Wibergs Stiftelse, Syskonen Svenssons Fond, Swedish Society of Medicine, Magn. Bergvalls Stiftelse, O.E. och Edla Johanssons Fond, Stiftelsen Lars Hiertas Minne, the Bank of Sweden Tercentenary Foundation, Tore Nilsons Foundation for Medical Research, Clas Groschinskys Minnesfond, Aage and Louis-Hansens Memorial Foundation, Novo Industry, W. och M. Lundgrens vetenskapsfond, The Royal Swedish Academy of Sciences, Svenska Sällskapet för Medicinsk Forskning, Funds of the Karolinska Institute and the Medical Faculty of Gothenburg University. P. Rorsman holds a postdoctoral fellowship at the Swedish Medical

Research Council and P. A. Smith was a recipient of a Royal Society European Exchange fellowship.

Original version received 25 January 1989 and accepted version received 16 October 1989.

REFERENCES

Arkhammar, P., T. Nilsson, P. Rorsman, and P.-O. Berggren. 1987. Inhibition of ATP-regulated K^+ channels precedes depolarization-induced increase in cytoplasmic free Ca^{2+} concentration in pancreatic β-cells. *Journal of Biological Chemistry.* 262:5448–5454.

Arkhammar, P., P. Rorsman, and P.-O. Berggren. 1986. Direct evidence for opposite effects of D-glucose and D-glyceraldehyde on cytoplasmic pH of mouse pancreatic β-cells. *Bioscience Reports.* 6:355–361.

Atwater, I., A. Goncalves, A. Herchuelz, P. Lebrun, W. J. Malaisse, E. Rojas, and A. Scott. 1984. Cooling dissociates glucose-induced insulin release from electrical activity and cation fluxes in rodent pancreatic islets. *Journal of Physiology.* 348:615–627.

Atwater, I., B. Ribalet, and E. Rojas. 1979. Mouse pancreatic β-cells: tetraethylammonium blockage of the potassium permeability increase induced by depolarization. *Journal of Physiology.* 288:561–574.

Bangham, J. A., and P. A. Smith. 1987. Nonconforming action potentials from isolated mouse islets of Langerhans. *Journal of Physiology.* 392:15P. (Abstr.)

Bangham, J. A., P. A. Smith, and P. C. Croghan. 1986. Modelling the β-cell electrical activity. *Advances in Experimental Medicine and Biology.* 211:265–278.

Bokvist, K., P. Rorsman, and P. A. Smith. 1990*a*. Effects of external tetraethylammonium ions and quinine on delayed rectifying K^+ channels in mouse pancreatic β-cells. *Journal of Physiology.* 411:311–325.

Bokvist, K., P. Rorsman, and P. A. Smith. 1990*b*. Block of ATP-regulated and Ca^{2+}-activated K^+ channels in mouse pancreatic β-cells by external tetraethylammonium and quinine. *Journal of Physiology.* 411:327–342.

Cook, D. L., M. Ikeuchi, and W. Y. Fujimoto. 1984. Lowering pH_i inhibits Ca^{2+}-activated K^+ channels in pancreatic B-cells. *Nature* 311:269–271.

Fenwick, E. M., A. Marty, and E. Neher. 1982. A patch-clamp study of bovine chromaffin cells and their sensitivity to acetylcholine. *Journal of Physiology.* 331:577–597.

Findlay, I., and M. J. Dunne. 1985. Voltage-activated Ca^{2+} currents in insulin-secreting cells. *FEBS Letters.* 189:281–285.

Grynkiewicz, G., M. Poenie, and R. Y. Tsien. 1985. A new generation of Ca^{2+} indicators with greatly improved fluorescence properties. *Journal of Biological Chemistry.* 260:3440–3450.

Hamill, O. P., A. Marty, E. Neher, B. Sakmann, and F. J. Sigworth. 1981. Improved patch-clamp techniques for high-resolution current recordings from cells and cell-free membrane patches. *Pflügers Archiv.* 391:85–100.

Heyer, C. B., and H. D. Lux. 1976. Control of the delayed outward potassium currents in bursting pace-maker neurones of the snail, *Helix pomatia. Journal of Physiology.* 262:349–382.

Hille, B. 1984. Ionic channels of excitable membranes. Sinauer Associates Inc., Sunderland, MA. pp. 23–57.

Horn, R., and A. Marty. 1988. Muscarinic activation of ionic currents measured by a new whole-cell recording method. *Journal of General Physiology.* 93:1–15.

Martell, A. E., and R. M. Smith. 1974. Critical stability constants. Vol. I: Amino Acids 469 pp. Vol. II: Amines. 415 pp. Plenum Publishing Corp., New York, NY. 469 pp.

Marty, A., and E. Neher. 1985. Potassium channels in cultured bovine adrenal chromaffin cells. *Journal of Physiology.* 367:117–141.

Meissner, H. P., J. C. Henquin, and M. Preissler. 1978. Potassium dependence of the membrane potential of pancreatic B-cells. *FEBS Letters.* 94:87–89.

Plant, T. D. 1988. Properties and calcium-dependent inactivation of calcium currents in cultured mouse pancreatic β-cells. *Journal of Physiology.* 404:731–747.

Ritchie, A. K. 1987. Two distinct calcium-activated potassium currents in a rat anterior pituitary cell line. *Journal of Physiology.* 385:591–609.

Rorsman, P., H. Abrahamsson, E. Gylfe, and B. Hellman. 1984. Dual effects of glucose on the cytosolic Ca^{2+} activity of mouse pancreatic B-cells. *FEBS Letters.* 170:196–200.

Rorsman, P., and G. Trube. 1985. Glucose dependent K^+-channels in pancreatic β-cells are regulated by intracellular ATP. *Pflügers Archiv.* 405:305–309.

Rorsman, P., and G. Trube. 1986. Calcium and delayed potassium currents in mouse pancreatic β-cells under voltage-clamp control. *Journal of Physiology.* 374:531–550.

Trube, G., P. Rorsman, and T. Ohno-Shosaku. 1986. Opposite effects of tolbutamide and diazoxide on ATP-dependent K^+ channels in mouse pancreatic β-cells. *Pflügers Archiv.* 407:493–499.

Velasco, J. M., and O. H. Petersen. 1987. Voltage-activation of high-conductance K^+ channel in the insulin-secreting cell line RINm5F is dependent on local extracellular Ca^{2+} concentration. *Biochimica et Biophysica Acta.* 896:305–310.

Zünkler, B. J., T. Ohno-Shosaku, and G. Trube. 1988. Forskolin-induced block of delayed rectifying K^+ channels in pancreatic β-cells is not mediated by cAMP. *Pflügers Archiv.* 411:613–619.